

Transient Isotopic Kinetic Study of the NO/H₂/O₂ (Lean de-NO_x) Reaction on Pt/SiO₂ and Pt/La–Ce–Mn–O Catalysts

Costas N. Costa and Angelos M. Efstathiou*

Department of Chemistry, University of Cyprus, P.O. Box 20537, CY 1678 Nicosia, Cyprus

Received: July 30, 2003; In Final Form: November 17, 2003

Steady-state isotopic transient kinetic analysis (SSITKA) coupled with temperature-programmed surface reaction (TPSR) methods and using in situ mass spectroscopy and DRIFTS have been applied for the first time to study essential mechanistic aspects of the NO/H₂/O₂ reaction at 140 °C under strongly oxidizing conditions over 0.1 wt % Pt/SiO₂ and 0.1 wt % Pt/La–Ce–Mn–O catalysts. The nitrogen-pathway of the reaction from NO to form N₂ and N₂O gas products was probed by following the ¹⁴NO/H₂/O₂ → ¹⁵NO/H₂/O₂ isotopic switch at 1 bar total pressure. It was found that the chemical structure of active intermediate NO_x species strongly depends on support chemical composition. In the case of the Pt/SiO₂ catalyst, the reaction route for N₂ and N₂O formation passes through the interaction of one reversibly and one irreversibly NO_x species chemisorbed on the Pt surface. On the other hand, in the case of a Pt/La–Ce–Mn–O catalyst, the reaction route passes through the interaction of two different in structure irreversibly chemisorbed NO_x species on the support. For the latter catalyst, the mechanism of the reaction must involve a hydrogen-spillover process from the Pt metal to the support surface. A surface coverage $\theta = 1.8$ (based on Pt metal surface) of active NO_x intermediate species was found for the Pt/La–Ce–Mn–O catalyst. A large fraction of it (81.5%) participates in the reaction path for N₂ formation, whereas in the case of Pt/SiO₂, this fraction was found to be 68.4% (active NO_x, $\theta = 0.65$). These important results provide an explanation for the lower N₂ reaction selectivity values observed on Pt/SiO₂ compared to Pt/La–Ce–Mn–O catalyst. Inactive adsorbed NO_x species (spectators) were found to accumulate on both Pt and support surfaces. It was found via the NO/H₂/¹⁶O₂ → NO/H₂/¹⁸O₂ isotopic switch that the reaction path from NO to form N₂O passes through the oxidation step of NO to NO₂ with the participation of gaseous O₂, where the extent of it depends on support chemical composition.

Introduction

The selective catalytic reduction (SCR) of NO by H₂ in the presence of strongly oxidizing conditions (>5 vol %) has attracted attention in the recent years.^{1–12} This is mainly due to the imposed stringent regulations of NO_x emissions from mobile and stationary sources with gas emission temperatures lower than 300 °C. It was first shown^{13,14} that H₂ can reduce NO_x at the lowest possible reaction temperatures. Today's great concern about the increasing emissions of carbon dioxide to the atmosphere will require the use of appropriate non-carbon-containing reducing chemical species for the development of new lean de-NO_x catalytic technologies.^{15–17} In addition, the facing problems of the currently used NH₃–SCR process in stationary power sources and chemical plants,¹⁸ e.g., the use of separate ammonia source and injection system, ammonia slip, toxicity and corrosiveness, and operational cost make desirable the replacement of ammonia with another reducing agent. Hydrogen –SCR could be considered as such an attractive alternative for the NH₃–SCR process.

For many conventional catalysts, the NO/H₂ reaction is strongly inhibited by oxygen due to the competition between adsorbed NO_x and oxygen species for activated adsorbed hydrogen species. Platinum supported on γ -Al₂O₃, SiO₂, and TiO₂ was found to be the most active for the NO/H₂/O₂ lean

de-NO_x reaction at temperatures lower than 200 °C compared to supported Rh and Pd catalysts.^{1–7} However, these catalytic systems present significantly low selectivity values toward N₂ formation ($S_{N_2} < 60\%$).^{3–5,7–9} Recent work from our laboratory^{8,9} has demonstrated that remarkably high N₂ selectivity values ($S_{N_2} = 80–92\%$) for the NO/H₂/O₂ reaction in the 100–250 °C range can be obtained over Pt supported on mixed oxidic and perovskite-type materials (e.g., Pt/Mn–Ce–O and Pt/La–Sr–Ce–O). In addition, a very wide operating temperature window and a positive effect of 5% H₂O in the feed stream on N₂ yield have been observed.^{8,9} It was shown that the catalytic behavior of the above-mentioned supported-Pt catalysts appear to be the best ever reported in the open literature for the NO/H₂/O₂ reaction system and in the presence of 5% H₂O in the feed stream.^{8,9}

Steady-state isotopic transient kinetic analysis (SSITKA),^{19–21} originally named steady-state tracing,²² has long been documented and widely accepted as the most powerful technique in performing in situ mechanistic studies for heterogeneous catalytic reactions, especially at 1 bar or higher pressures. SSITKA consists of following the composition of the outlet of a reactor initially at steady state when one of the reactants is suddenly replaced by the same molecular species but with one of its atoms replaced by one of its stable isotopes. Recent review papers on the technique and its applications to several catalytic reactions have appeared.^{19–21,23} In particular, SSITKA experiments on de-NO_x reactions have been published for NO/NH₃/

* To whom correspondence should be addressed. Tel: +35722-892776. Fax: +35722-892801. E-mail: efstath@ucy.ac.cy.

O₂ over V₂O₅/TiO₂,^{19,24} NO/CH₄/O₂ over Pd/TiO₂,²⁵ NO/C₃H₆/O₂ over Pt/SiO₂,^{26,27} and NO/H₂ over Pt/SiO₂ catalysts.^{28,29}

In a recent work, Burch et al.³⁰ have used the SSITKA technique (use of ¹⁵NO) to study the NO/H₂/O₂ reaction mechanism over a Pt/SiO₂ catalyst. This work provided for the first time significant information about the concentration of the adsorbed active intermediate NO_x species formed during reaction conditions and aspects of the reaction pathways of N₂ and N₂O formation. However, neither experimental evidence was provided about the chemical structure of the active NO_x species nor any information about the existence of likely spectator adsorbed NO_x species. Also, no information has yet been provided concerning the effect of support on the mechanism of reaction at hand over supported-Pt catalysts.

In the present work, SSITKA experiments with the use of both ¹⁵NO and ¹⁸O₂ stable isotopes were conducted with in situ mass spectrometry and diffuse reflectance infrared fourier transform spectroscopy (DRIFTS) on the 0.1 wt % Pt/La_{0.5}Ce_{0.5}MnO₃ and 0.1 wt % Pt/SiO₂ catalyst surfaces. The purpose of these experiments was the determination of the chemical structure of adsorbed active and inactive (spectator) NO_x species and the measurement of their surface coverage under NO/H₂/O₂ reaction conditions. Based on these results, a critical comparison of the effects of support chemical composition on key aspects of the reaction mechanism was made.

It is reported for the first time that important aspects of the mechanism of N₂ and N₂O formation of the NO/H₂/O₂ reaction strongly depend on support chemical composition. In particular, it was found that the support chemical composition has a strong influence on the kinds of active intermediate NO_x species formed on the Pt metal and the support surface. This result then determines the N₂ selectivity of the reaction (N₂O is the other N-containing gas product formed). The role of gaseous oxygen in the reaction path has also been probed. It was found that oxygen atoms of the di-oxygen gas participate in the production of N₂O in an extent that depends on the support chemical composition.

Experimental Section

Catalyst Preparation and Characterization. The La_{0.5}Ce_{0.5}MnO₃ solid was prepared using the ceramic method as follows: calculated amounts of La(NO₃)₃·6H₂O (Merck), Mn(NO₃)₃·9H₂O (Merck), and CeO₂ (Aldrich) were mixed thoroughly in an agate mortar and heated slowly up to 400 °C for nitrate decomposition. At the end of this step (no visible NO₂ fumes), the system was further heated at 1 bar for 4 h at 900 °C. Then, the mixture was removed from the furnace, cooled, and, after grinding, heated again for another 4 h at 1050 °C. The sample was then slowly cooled to room temperature and stored for further use. It is mentioned that the notation La_{0.5}Ce_{0.5}MnO₃ indicates just the nominal composition of the solid. This has nothing to do with particular crystal phases existing in each sample.

The supported metal catalysts (0.1 wt % Pt/La_{0.5}Ce_{0.5}MnO₃ and 0.1 wt % Pt/SiO₂) were prepared by the incipient wetness impregnation method using the H₂Pt(IV)Cl₆ (Aldrich) precursor. The SiO₂ support was supplied from Aldrich (99.9% purity). After impregnation and drying (overnight at ~120 °C), the catalyst samples were calcined in air at 600 °C for 2 h prior to use. The crystal structure of the prepared La_{0.5}Ce_{0.5}MnO₃ solid was checked by XRD analyses using a SIEMENS Diffract 500 system employing Cu Kα radiation (λ = 1.5418 Å). The dispersion of Pt in the catalyst was determined by H₂ chemisorption according to the following procedure and taking into

TABLE 1: Sequential Step Changes of Gas Flow during Transient Isotopic Experiments Performed on 0.1 wt % Pt/La_{0.5}Ce_{0.5}MnO₃ and 0.1 wt % Pt/SiO₂ Catalysts

experiment code	sequence of step changes of gas flow over the catalyst sample
A	¹⁴ NO/H ₂ /O ₂ /Ar/He (30 min, 140 °C) → <u>¹⁵NO/H₂/O₂/He (140 °C, t)</u> (SSITKA experiment)
B	¹⁴ NO/H ₂ /O ₂ /Ar/He (30 min, 140 °C) → ¹⁵ NO/He (15 min, 140 °C) → He (5 min, 140 °C) → cool quickly to room temperature → <u>TPSR in 10% H₂/He</u>
C	NO/H ₂ / ¹⁶ O ₂ /Ar/He (30 min, 140 °C) → <u>NO/H₂/¹⁸O₂/He (140 °C, t)</u> (SSITKA experiment)

account the observations made by Gatica et al.³¹ After calcination at 600 °C for 2 h in a 20% O₂/He gas mixture, the catalyst sample was reduced in H₂ (1 bar) at 300 °C for 2 h. Following this step, the feed was changed to He and the temperature was increased to 500 °C in He flow and kept at this temperature until no hydrogen desorption was observed. A possible hydrogen spillover that might have taken at 300 °C was eliminated by the latter procedure. The reactor was then quickly cooled in He flow to 25 °C and the feed was changed to a 1% H₂/He gas mixture for 30 min. Following the latter chemisorption step, the feed was changed to He and kept at 25 °C for 10 min before the temperature of the catalyst was increased to 600 °C at the rate of 30 °C/min to carry out a TPD experiment. From the amount of hydrogen desorbed, the amount of Pt in the sample and assuming H/Pt_s = 1:1 the dispersion of Pt was estimated.

Transient Mass Spectrometry. Transient isotopic and temperature-programmed reaction (TPR) experiments were conducted in a specially designed transient flow-system and a quartz microreactor that have been recently described.^{32,33} For transient experiments, 0.15 g of catalyst sample was used and the total flow rate was 30 scc/min. Chemical analysis of the gas effluent stream of reactor during transient experiments was performed with an on line quadrupole mass spectrometer (Omnistar, Balzers). The latter was equipped with a fast response inlet capillary/leak valve (SVI 050, Balzers) and data acquisition systems. The gaseous responses obtained by mass spectrometry were calibrated against standard mixtures.

Before any measurements were taken, the supported-Pt catalyst was calcined in 5% O₂/He for 2 h at 600 °C followed by reduction in 10% H₂/He gas mixture at 300 °C for 2 h. The feed was then switched to pure He at 300 °C for 15 min and the reactor was cooled to the appropriate temperature of the experiment to be followed. Table 1 describes the necessary sequence of steps performed for each kind of isotopic transient experiment presented in this work. The underlined step is that during which measurements by on line mass spectrometry were recorded.

The SSITKA (steady-state isotopic transient kinetic analysis) experiments involved the switch of the feed NO/H₂/O₂/Ar/He to an equivalent in composition ¹⁵NO/H₂/O₂/He or NO/H₂/¹⁸O₂/He gas mixture after steady state was achieved. The argon (Ar) gas was used as a tracer, the decay of which was used to monitor the gas phase hold-up of the system.¹⁹ Following the switch ¹⁴NO/H₂/O₂/Ar/He → ¹⁵NO/H₂/O₂/He, the mass numbers (*m/z*) 2, 28, 29, 30, 31, 32, 40, 44, and 45 used for H₂, ¹⁴N₂, ¹⁴N¹⁵N, ¹⁴NO, ¹⁵NO, O₂, Ar, ¹⁴N₂O, and ¹⁴N¹⁵NO, respectively, were continuously monitored. In the case of the switch NO/H₂/¹⁶O₂/Ar/He → NO/H₂/¹⁸O₂/He, the mass numbers (*m/z*) 2, 30, 32, 34, 36, 40, 44, and 46 used for H₂, NO, ¹⁶O₂, ¹⁶O¹⁸O, ¹⁸O₂, Ar, N₂¹⁶O, and N₂¹⁸O, respectively, were continuously monitored. Details of the mass spectrometry analyses of the reactor gas effluent have been reported.^{8,32} It should be noted that neither

NH₃ nor any NO₂ gas product was measured under the present NO/H₂/O₂/He catalytic reaction conditions.

The reaction mixture contained 0.25% NO, 1% H₂, 5% O₂, and He as balance gas in all experiments performed. In the case that Ar was used as a tracer gas in the reaction mixture, 1% He was replaced with Ar. The ¹⁵NO/He gas mixture used in expt. B described in Table 1 contained 0.25% ¹⁵NO gas and it was prepared by using a 1 mol % ¹⁵NO/He isotopic mixture (ISOTEC, Inc. U.S.A.). The NO/H₂/¹⁸O₂/He gas mixture used in the DRIFTS/SSITKA experiments described in Table 1 (expt. C) contained 2 mol % ¹⁸O₂ isotope gas and it was prepared by using a 3 mol % ¹⁸O₂ isotopic mixture (ISOTEC, Inc. U.S.A., 97 at. % ¹⁸O).

In Situ Transient DRIFTS. Diffuse reflectance infrared Fourier transform (DRIFT) spectra were recorded on a Perkin-Elmer GX FTIR spectrophotometer at a resolution of 1 cm⁻¹ and using a high-temperature/high-pressure temperature controllable DRIFTS cell (Spectra Tech) equipped with ZnSe IR windows. About 30 mg of catalyst sample in powder form was used for each experiment. The total flow rate was kept constant at 50 scc/min. Before any measurements were taken, the supported-Pt catalyst was pretreated in situ in 5% O₂/He for 2 h at 600 °C followed by treatment in 10% H₂/He gas mixture at 300 °C for 2 h. The feed was then switched to pure Ar at 300 °C for 15 min and the sample was cooled to the appropriate temperature of the experiment to be followed. For FTIR single-beam background subtraction, the spectrum of the catalyst (in reduced state) was taken in Ar flow. FTIR spectra were collected at the rate of 1 scan/s at 1 cm⁻¹ resolution in the 800–3000 cm⁻¹ range and the averaged spectrum was then recorded. All spectra were analyzed by using the instrument's Spectrum for Windows software provided.

Results

Catalyst Characterization. The Pt dispersion, *D*(%) ($\mu\text{mol Pt}_s/\mu\text{mol Pt} \times 100$), of the investigated 0.1 wt % Pt/La_{0.5}Ce_{0.5}MnO₃ and 0.1 wt % Pt/SiO₂ catalysts measured according to the procedure given previously in the Experimental Section was found to be about 90% for each catalyst resulting in 4.6 $\mu\text{mol Pt}_s/\text{g}$ of catalyst. X-ray diffraction analyses of the La_{0.5}Ce_{0.5}MnO₃ solid support have indicated that this solid material consisted of three crystal phases, namely, LaMnO₃ (perovskite-like structure), CeO₂, and MnO₂. The BET surface area of this mixed oxide solid support was found to be about 5 m²/g. It is expected that impregnation of 0.1 wt % Pt onto La_{0.5}Ce_{0.5}MnO₃ solid support resulted in a mixture of supported-Pt crystallites within the pore system of LaMnO₃, CeO₂, and MnO₂ crystal phases.

In Situ DRIFTS Studies. The chemical structure of the adsorbed intermediate NO_x species formed on the surface of 0.1 wt % Pt/La_{0.5}Ce_{0.5}MnO₃ and 0.1 wt % Pt/SiO₂ catalysts during the NO/H₂/O₂ reaction at 140 °C was studied by in situ DRIFTS. The composition of the feed gas stream used consisted of 0.25 vol % NO, 1 vol % H₂, 5 vol % O₂, and Ar as a carrier gas. The assignment of the IR absorption bands was made based on the literature.^{34–45} Table 2 presents the chemical structure and absorption bands (stretching mode) of all of the important adsorbed NO_x species observed during the present DRIFTS studies and others reported in the literature.

Figure 1 shows IR bands in the 1000–2200 cm⁻¹ range recorded after 30 min of NO/H₂/O₂ reaction at 140 °C over the Pt/La_{0.5}Ce_{0.5}MnO₃ (Figure 1a) and Pt/SiO₂ (Figure 1b) catalysts. Four main IR bands were observed in the case of the Pt/La_{0.5}Ce_{0.5}MnO₃ catalyst (Figure 1a). The band recorded at 2220 cm⁻¹

TABLE 2: Chemical Structures and Absorption Bands (Stretching Mode) of Various Adsorbed NO_x Species on Supported-Pt Catalysts^{34–45 a}

Species	Structure	Wavenumber (cm ⁻¹)
Nitric Oxide	NO (g)	1840
Nitrogen hypoxide Nitrosyls on support	M-N ₂ O M-NO ⁺ , M-NO ₂ ⁺	~2220
Nitrogen Dioxide	M-NO ₂ ^{δ+} , M-NO ^{δ+}	2100–2200
Nitrosyls on Pt	NO-Pt _{ox} NO-Pt _{red} NO ^{δ+} -Pt	~1840 ~1800 1900–2000
Bridged or bent NO on Pt	Pt _n -NO	1700–1500 (depending on n)
Unidentate Nitrates		1470–1540
		1480–1560
Bidentate Nitrates		1620–1660
		1520–1610
Nitritos		1420–1435
Chelating nitrite (NO ₂ ⁻)		1325, 1100–1300
Dimeric NO, N ₂ O ₂ ⁿ⁻ (n=1,2)		1050–1375

^a M: Metal cation on the support surface.

(Figure 1a) corresponds to adsorbed nitrosyls (NO⁺ and NO₂⁺) on the support.^{34–36} Strong evidence for the presence of M-NO₂⁺ is provided by the ¹⁸O₂ SSITKA experiments to be presented later on. There is no evidence for the formation of adsorbed N₂O since no IR band was observed at 1285 cm⁻¹ that corresponds to the bending mode of chemisorbed N₂O on the support.³⁷ The IR band at 1700 cm⁻¹ corresponds to bridged or bent NO on Pt.^{37,38} The shoulder recorded at 1620 cm⁻¹ can be attributed to bidentate nitrates on Pt,^{39,40} but also molecularly adsorbed water.^{41,42} Deconvolution (Gaussian peak shape) of the complex IR band observed in the 1300–1600 cm⁻¹ range (see inset graph, Figure 1a) results in four new IR bands at 1540, 1520, 1470, and 1410 cm⁻¹.

The IR band assignments in the 1300–1600 cm⁻¹ range to be discussed next are based on the following observations: (a) the low Pt loading used in the present catalysts (0.1 wt %), (b) the range of IR bands in which the various kinds of NO_x species appear (see Table 2), (c) the integral band intensities and bandwidths shown in the inset of Figure 1a, and (d) the support chemical composition. The IR band at 1540 cm⁻¹ corresponds to bidentate nitrates on the support,⁴³ that at 1520 cm⁻¹ to unidentate nitrates on Pt,⁴¹ that at 1470 cm⁻¹ to *unidentate nitrates on the support*,⁴³ and that at 1410 cm⁻¹ to *nitritos on the support*.⁴³ Finally, the IR band recorded at 1250 cm⁻¹ corresponds to chelating nitrite (NO₂⁻) and/or N₂O₂ⁿ⁻ (n = 1 and 2) on the support.^{40,44,45}

A significantly different FTIR spectrum was recorded in the case of Pt/SiO₂ catalyst (Figure 1b). As shown in Figure 1b, no

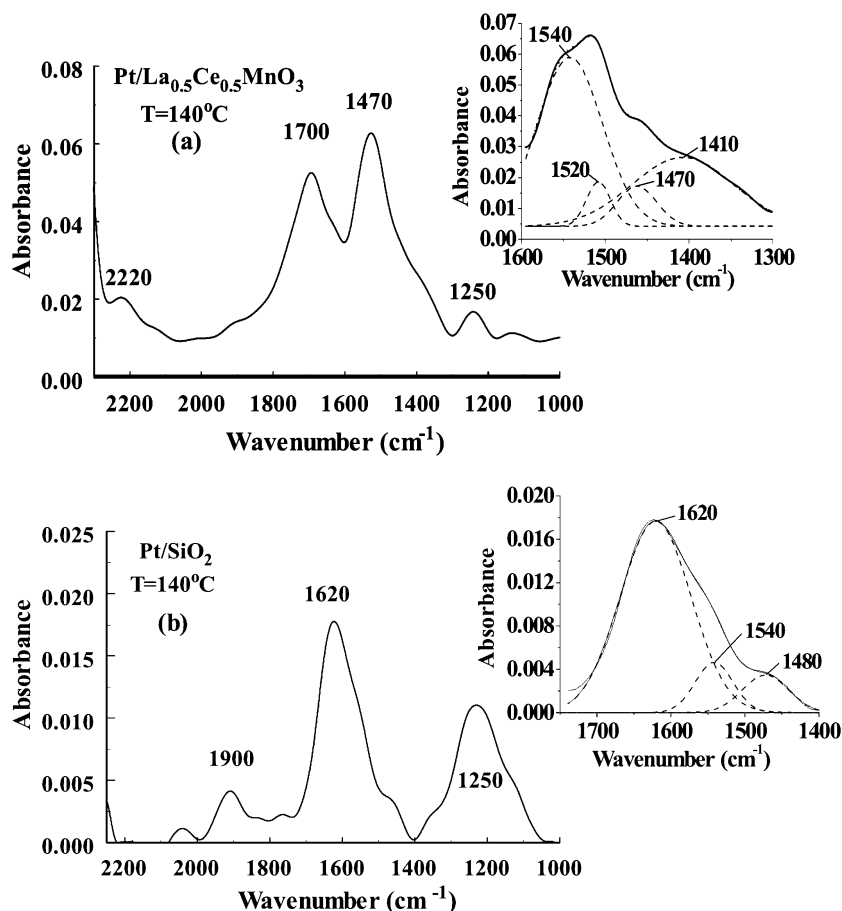


Figure 1. In situ DRIFTS spectra recorded over the 0.1 wt % Pt/La_{0.5}Ce_{0.5}MnO₃ (a) and 0.1 wt % Pt/SiO₂ (b) catalysts after 30 min of NO/H₂/O₂ reaction at 140 °C. Inset graph: Deconvolution of the DRIFTS spectrum recorded in the 1600–1300 cm⁻¹ range. Feed gas composition: H₂ = 1.0%, NO = 0.25%, O₂ = 5%, Ar as balance gas.

IR bands were recorded at 2220, 1700, and 1470 cm⁻¹, whereas a small IR band was recorded at 1900 cm⁻¹, not observed in the case of the Pt/La_{0.5}Ce_{0.5}MnO₃ catalyst (Figure 1a). The latter IR band is attributed to adsorbed nitrosyls on Pt.⁴² Deconvolution (Gaussian peak shape) of the IR band observed in the 1400–1750 cm⁻¹ range (see inset graph, Figure 1b) results in two new IR bands at 1540 and 1480 cm⁻¹, besides the initial one at 1620 cm⁻¹. As previously discussed and according to Table 2, the IR bands at 1620, 1540 and 1480 cm⁻¹ are assigned to bidentate nitrates on Pt, bidentate nitrates on silica, and unidentate nitrates on Pt, respectively. The IR band at 1250 cm⁻¹ corresponds to chelating nitrite (NO₂⁻) and/or N₂O₂ⁿ⁻¹ (*n* = 1 and 2) species adsorbed on the SiO₂ support (Table 2). It is noted that adsorbed NO_x species on SiO₂ were also probed by various kinds of transient experiments following NO/H₂/O₂ reaction at 140 °C over the Pt/SiO₂ catalyst.⁸ It should also be noted that no NO_x species were observed following NO/H₂/O₂ reaction for 30 min at 140 °C over the SiO₂ support itself. Thus, the NO_x adsorbed species observed with FTIR and assigned to silica support must be located within the Pt–SiO₂ interface region.

The chemical structure of the active adsorbed NO_x species participating in the reaction path of the NO/H₂/O₂ lean de-NO_x reaction was determined by performing steady-state tracing (SSITKA) experiments. The experimental procedure was as follows. Initially, FTIR spectra were recorded after 30 min of reaction in ¹⁴NO/H₂/O₂ at 140 °C. The reaction feed stream was then switched to the equivalent isotopic ¹⁵NO/H₂/O₂ gas mixture, and FTIR spectra were recorded after 30 min of continuous reaction.

Figure 2 shows the FTIR spectra recorded over the Pt/La_{0.5}Ce_{0.5}MnO₃ (Figure 2a) and Pt/SiO₂ (Figure 2b) catalysts 30 min before (—) and after (---) the switch ¹⁴NO/H₂/O₂/He → ¹⁵NO/H₂/O₂/He was made at 140 °C. The IR bands that are shifted to lower wavenumbers after the isotopic switch (¹⁵N–O vs ¹⁴N–O stretching vibrational mode) correspond to the active adsorbed intermediate NO_x species of the NO/H₂/O₂ reaction that eventually forms N₂ and N₂O gas products. However, the likelihood for the presence of inactive but exchangeable NO_x species with gaseous ¹⁵NO cannot be excluded. The shift of IR bands shown in Figure 2 by 30–50 cm⁻¹ is consistent with the theory and the experimental work of Beutel et al.⁴⁶

After an appropriate band deconvolution (see inset graph in Figure 1a) was made, only two IR bands are shifted to lower wavenumbers in the case of Pt/La_{0.5}Ce_{0.5}MnO₃ catalyst (Figure 2a). The first band recorded at 2220 cm⁻¹ and shifted to 2170 cm⁻¹ corresponds to nitrosyls on the support. The second IR band recorded at 1540 cm⁻¹ and shifted to 1500 cm⁻¹ is attributed to bidentate nitrates also on the support as previously discussed. Therefore, the two active intermediate NO_x species formed on the Pt/La_{0.5}Ce_{0.5}MnO₃ catalyst during NO/H₂/O₂ reaction are the nitrosyls and bidentate nitrates both present on the support surface.

A completely different result was obtained in the case of the Pt/SiO₂ catalyst (Figure 2b). After a band deconvolution was made in the 1700–1400 cm⁻¹ range (see inset of Figure 1b), the two active NO_x species observed on Pt/SiO₂ correspond to adsorbed nitrosyls and unidentate nitrates on the Pt surface.

To gain more fundamental information concerning key aspects of the mechanism of the reaction and particularly to

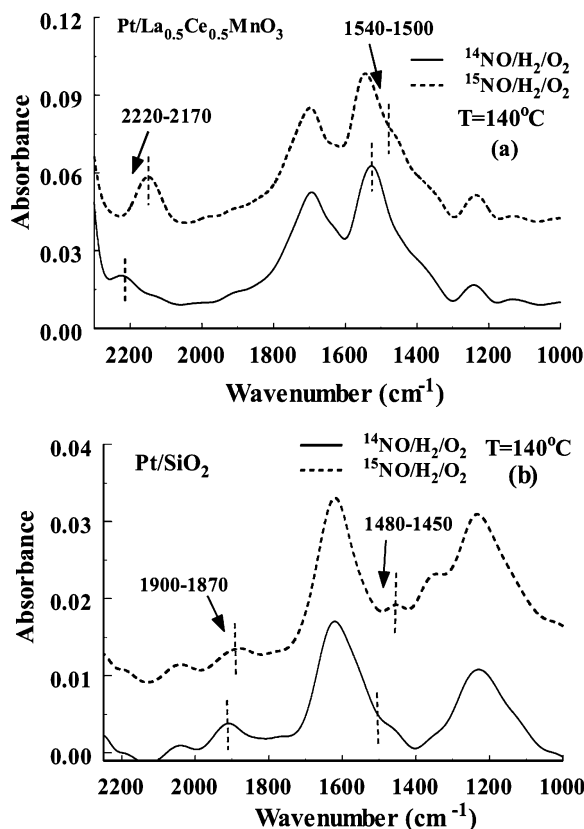


Figure 2. In situ DRIFTS spectra recorded over the 0.1 wt % Pt/La_{0.5}Ce_{0.5}MnO₃ (a) and 0.1 wt % Pt/SiO₂ (b) catalysts after 30 min of ¹⁴NO/H₂/O₂/Ar reaction (—) at 140 °C, and after 30 min following the isotopic switch ¹⁴NO/H₂/O₂/Ar → ¹⁵NO/H₂/O₂/Ar (---) at 140 °C. Feed composition: H₂ = 1.0%, NO = 0.25%, O₂ = 5%, Ar as balance gas.

identify whether the active adsorbed NO_x species formed during the NO/H₂/O₂ reaction reversibly interact with gaseous NO (exchangeable NO_x species), the following experiment has been designed. After 30 min of ¹⁴NO/H₂/O₂/Ar reaction at 140 °C, the reaction feed was switched to ¹⁵NO/Ar and the FTIR spectrum was recorded after 15 min on stream. The purpose of the latter switch was to stop the reaction and simultaneously exchange the reversibly chemisorbed NO_x species with ¹⁵NO from the gas phase.

Figure 3 shows the FTIR spectra recorded over the Pt/La_{0.5}Ce_{0.5}MnO₃ (Figure 3a) and Pt/SiO₂ (Figure 3b) catalysts 30 min after reaction in ¹⁴NO/H₂/O₂/Ar and 15 min after the switch ¹⁴NO/H₂/O₂/Ar → ¹⁵NO/Ar was made at 140 °C. The IR bands that are shifted to lower wavenumbers (after appropriate band deconvolution was performed) following the isotopic switch correspond to the reversibly chemisorbed intermediate NO_x species formed during NO/H₂/O₂ reaction. After deconvolution of the band in the 1300–1600 cm⁻¹ range, only the original IR band at 1520 cm⁻¹ is shifted to 1470 cm⁻¹. As mentioned above, this IR band corresponds to unidentate nitrates on the Pt surface (Table 2). Therefore, it can be said that among the two active intermediate NO_x species which are formed on the Pt/La_{0.5}Ce_{0.5}MnO₃ catalyst surface during NO/H₂/O₂ reaction (Figure 2a) none is considered as reversibly chemisorbed. Similarly, as shown in Figure 3b, for the two active intermediate NO_x species that are formed on Pt/SiO₂ catalyst (Figure 2b), only the nitrosyls on Pt are considered as reversibly chemisorbed species.

It is noted that the FTIR spectra shown in Figure 3a are somehow different in shape when compared to the corresponding ones of Figures 1a and 2a. This is due to the change in the intensities of the various adsorbed NO_x species after continuous

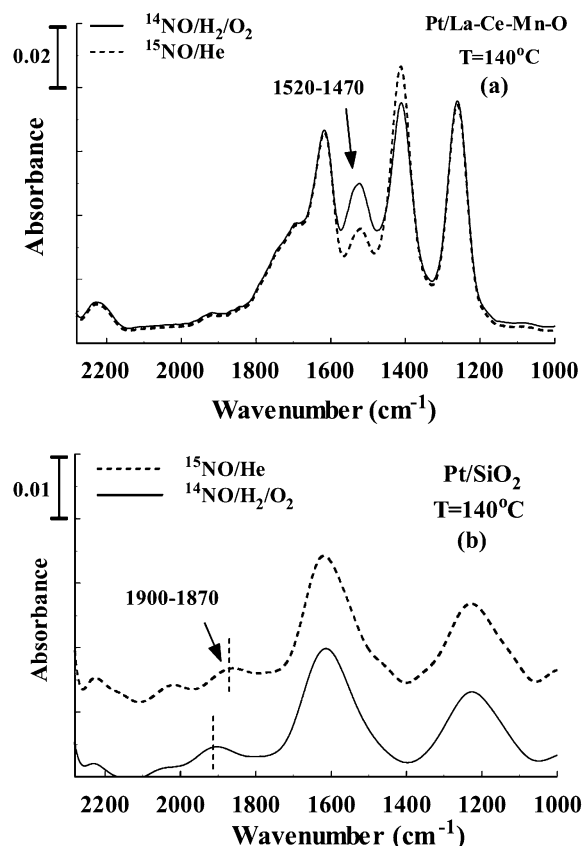


Figure 3. In situ DRIFTS spectra recorded over the 0.1 wt % Pt/La_{0.5}Ce_{0.5}MnO₃ (a) and 0.1 wt % Pt/SiO₂ (b) catalysts after 30 min of ¹⁴NO/H₂/O₂/Ar reaction (—) and after 15 min following the switch ¹⁴NO/H₂/O₂/Ar → ¹⁵NO/Ar (---) at 140 °C. Feed composition: H₂ = 1.0%, NO = 0.25%, O₂ = 5%, Ar as balance gas. Isotopic feed composition: ¹⁵NO = 0.25%, Ar as balance gas.

exposure of the same catalyst sample in various gas atmospheres in the DRIFTS cell. However, the chemical structure of all adsorbed NO_x species recorded remained always the same.

Transient Mass Spectrometry. The surface coverage of the active adsorbed intermediate NO_x species found in the nitrogen-pathway of the NO/H₂/O₂ reaction at 140 °C and which are responsible for the production of N₂ and N₂O were determined by SSITKA experiments (use of ¹⁵NO). Figures 4 and 5 present the transient isotopic response curves of N₂ (a) and N₂O (b) obtained after the switch ¹⁴NO/H₂/O₂/Ar/He → ¹⁵NO/H₂/O₂/He was made at 140 °C (expt. A, Table 1) over the Pt/La_{0.5}Ce_{0.5}MnO₃ (Figure 4) and Pt/SiO₂ (Figure 5) catalyst, respectively. The results are expressed in terms of the dimensionless concentration, Z, which represents the fraction of the ultimate change (giving Z = 0) as a function of time. Thus, Z is defined by

$$Z(t) = \frac{(y(t) - y_{\infty})}{(y_0 - y_{\infty})} \quad (1)$$

where the subscripts 0 and ∞ refer to the values of y (mole fraction) just before ($t = 0$) and long after the isotopic switch ($t \rightarrow \infty$). The decay of Ar gas concentration shown in Figures 4 and 5 was used to monitor the gas phase hold-up of the system.^{19–21} As seen in Figure 4, the only ¹⁵N-containing isotopic products are ¹⁴N¹⁵N (Figure 4a) and ¹⁴N¹⁵NO (Figure 4b) in the case of Pt/La_{0.5}Ce_{0.5}MnO₃ catalyst. No ¹⁴N₂ isotopic gas is practically observed (note the overlap of Ar and ¹⁴N₂ transient response curves). A similar result was also obtained

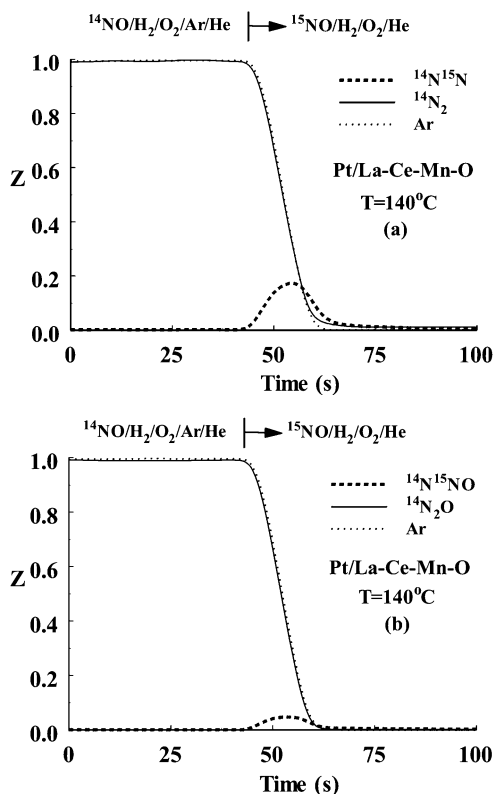


Figure 4. Transient response curves of $^{14}\text{N}_2$, $^{14}\text{N}^{15}\text{N}$, and Ar (a) and $^{14}\text{N}_2\text{O}$, $^{14}\text{N}^{15}\text{NO}$, and Ar (b) obtained following the isotopic switch $^{14}\text{NO}/\text{H}_2/\text{O}_2/\text{Ar}/\text{He}$ (30 min) \rightarrow $^{15}\text{NO}/\text{H}_2/\text{O}_2/\text{He}$ (t) at 140 °C (expt. A, Table 1) over the 0.1 wt % Pt/La_{0.5}Ce_{0.5}MnO₃ catalyst. Feed gas composition: H₂ = 1.0%, NO = 0.25%, O₂ = 5%, Ar = 1%, He as balance gas.

in the case of Pt/SiO₂ catalyst (Figure 5). The amount of active NO_x species that participate in the reaction path to form N₂ and N₂O is calculated by the integration of the corresponding transient response curves of $^{14}\text{N}^{15}\text{N}$ and $^{14}\text{N}^{15}\text{NO}$. In the case of Pt/La_{0.5}Ce_{0.5}MnO₃ catalyst, this amount is found to be 8.10 μmol N/g. It is also found that 81.5% of this amount (6.6 μmol N/g) leads to the formation of N₂, whereas 18.5% (1.5 μmol N/g) leads to the formation of N₂O. A significantly smaller amount of active NO_x species (3.04 μmol N/g) is found in the case of Pt/SiO₂ (Figure 5) compared to Pt/La_{0.5}Ce_{0.5}MnO₃ catalyst. Only 68.4% (2.08 μmol N/g) of this amount was found to lead to N₂ formation, whereas the remaining of it leads to the formation of N₂O (0.96 μmol N/g). The amounts of active NO_x species calculated based on the SSITKA experimental results (Figures 4 and 5) are given in Table 3. The last column of Table 3 gives also the amount of total adsorbed NO_x species in terms of surface coverage, θ , the latter quantity based on the exposed surface Pt atoms (μmol Pt_s/g). For adsorbed NO_x species on support sites, the parameter θ has no physical meaning. However, estimated values of θ greater than unity signify the fact that part of the measured NO_x species cannot be found on the Pt surface.

The surface coverage of the active NO_x species formed during the NO/H₂/O₂ reaction and which are reversibly chemisorbed (exchangeable) on the catalyst surface was determined by the combination of an isotopic exchange (use of ^{15}NO) and temperature-programmed surface reaction (TPSR) in H₂ experiment (expt. B, Table 1). It is noted that the underlined step in Table 1 is that during of which measurements by on line mass spectrometry were recorded. Figure 6 shows the transient response curves of ^{15}NO , $^{14}\text{N}_2\text{O}$, and $^{14}\text{N}^{15}\text{N}$ obtained over the

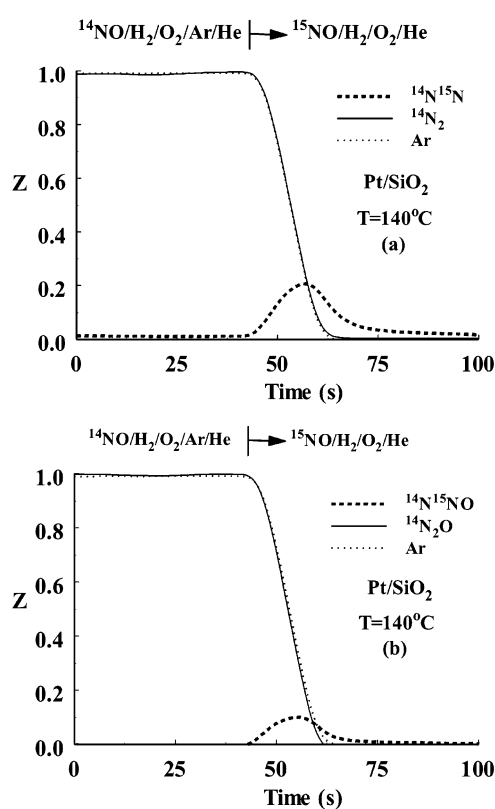


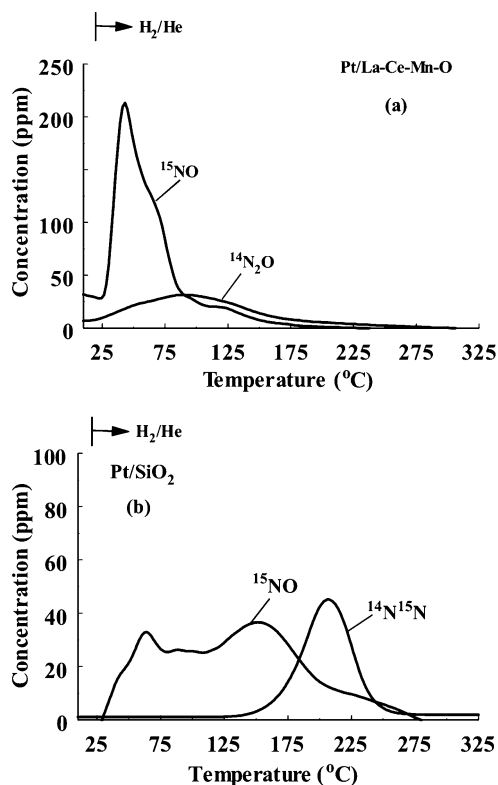
Figure 5. Transient response curves of $^{14}\text{N}_2$, $^{14}\text{N}^{15}\text{N}$, and Ar (a) and $^{14}\text{N}_2\text{O}$, $^{14}\text{N}^{15}\text{NO}$, and Ar (b) obtained following the isotopic switch $^{14}\text{NO}/\text{H}_2/\text{O}_2/\text{Ar}/\text{He}$ (30 min) \rightarrow $^{15}\text{NO}/\text{H}_2/\text{O}_2/\text{He}$ (t) at 140 °C (expt. A, Table 1) over the 0.1 wt % Pt/SiO₂ catalyst. Feed gas composition: H₂ = 1.0%, NO = 0.25%, O₂ = 5%, Ar = 1%, He as balance gas.

Pt/La_{0.5}Ce_{0.5}MnO₃ (Figure 6a) and Pt/SiO₂ (Figure 6b) catalysts for the above-referenced isotopic experiment. In the case of the Pt/La_{0.5}Ce_{0.5}MnO₃ catalyst (Figure 6a), a sharp ^{15}NO peak is observed at 45 °C with a shoulder at the falling part of it and a tail out to 175 °C. On the contrary, a smaller broad $^{14}\text{N}_2\text{O}$ peak is obtained in the 25–275 °C range. The presence of the $^{14}\text{N}_2\text{O}$ peak strongly suggests that formation of N₂O is the result of the reduction by H₂ of only nonexchangeable NO_x species. A significantly different TPSR profile is obtained in the case of the Pt/SiO₂ catalyst (Figure 6b), where transient response curves of ^{15}NO and $^{14}\text{N}^{15}\text{N}$ are observed. A desorption peak of ^{15}NO under H₂ flow is obtained at 70 °C and a broader one at 150 °C. In addition, a $^{14}\text{N}^{15}\text{N}$ peak is observed at 215 °C. The latter result strongly suggests that N₂ production from the reduction by H₂ of NO_x species requires the interaction of two different adsorbed NO_x species, one of which is reversibly chemisorbed whereas the other one is not. The amounts of produced gaseous species shown in Figure 6 and the equivalent amount of adsorbed NO_x species are given in Table 3 (expt. B).

To gather information for the role of O₂ in the NO/H₂/O₂ lean de-NO_x reaction mechanism, similar SSITKA experiments with the use of $^{18}\text{O}_2$ were conducted at 140 °C. Figure 7 presents the transient response curves of N₂¹⁸O, N₂¹⁶O, and Ar obtained on Pt/La_{0.5}Ce_{0.5}MnO₃ (Figure 7a) and Pt/SiO₂ (Figure 7b) catalysts after the switch NO/H₂/¹⁶O₂/Ar/He \rightarrow NO/H₂/¹⁸O₂/He was made at 140 °C (expt. C, Table 1). As seen in Figure 7, the concentration of N₂¹⁶O produced by both catalysts is reduced after the isotopic switch, whereas the continuous evolution of N₂¹⁸O is noticed. The sum of the steady-state concentrations of N₂¹⁸O and N₂¹⁶O formed under reaction in

TABLE 3: Amount of N-Containing Species Desorbed ($\mu\text{mol/g}_{\text{cat}}$) during Various Kinds of Transient Isotopic Experiments as a Function of Catalyst Composition

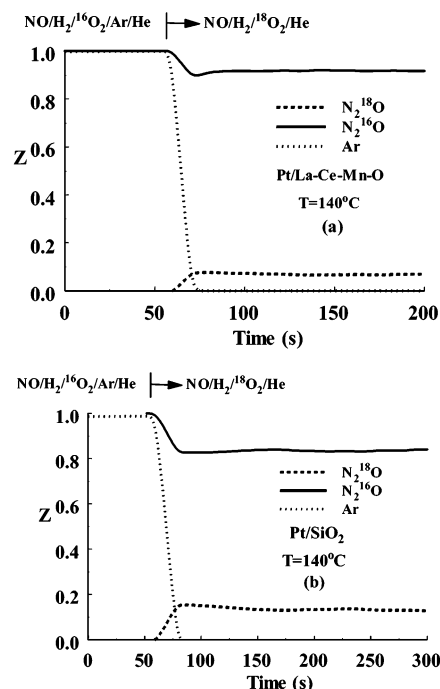
catalyst sample	expt. (Table 1)	$^{14}\text{N}^{15}\text{N}$	$^{14}\text{N}^{15}\text{NO}$	$^{14}\text{N}_2^{16}\text{O}$	^{15}NO	total adsorbed NO_x species ($\mu\text{mol/g}$)
Pt/La _{0.5} Ce _{0.5} MnO ₃	A	3.3	0.75			8.10 ($\theta = 1.74$)
	B			3.9	5.7	13.5 ($\theta = 2.9$)
Pt/SiO ₂	A	1.04	0.48			3.04 ($\theta = 0.65$)
	B	1.0			1.4	3.4 ($\theta = 0.74$)

**Figure 6.** Transient response curves of ^{15}NO , $^{14}\text{N}^{15}\text{N}$, and $^{14}\text{N}_2\text{O}$ obtained during TPSR in 10% H_2/He flow on the 0.1 wt % Pt/La_{0.5}Ce_{0.5}MnO₃ (a) and 0.1 wt % Pt/SiO₂ (b) catalysts according to the sequence of steps described in expt. B of Table 1. $Q_{\text{H}_2/\text{He}} = 30 \text{ cm}^3/\text{min}$; $\beta = 30 \text{ }^\circ\text{C}/\text{min}$.

the isotopic gas mixture is the same as the steady-state concentration of N_2^{16}O formed under the nonisotopic gas mixture ($Z = 1.0$). It is also important to point out that the decrease in the concentration of N_2^{16}O observed in the case of Pt/SiO₂ (Figure 7b) is twice larger than that observed in the case of Pt/La_{0.5}Ce_{0.5}MnO₃ catalyst (Figure 7a). In particular, the concentration of N_2^{16}O was found to decrease by approximately 17% after 4 min of the isotopic switch over the Pt/SiO₂ catalyst. The latter results strongly indicate that participation of gaseous O_2 toward N_2O formation in the $\text{NO}/\text{H}_2/\text{O}_2$ reaction is more substantial on Pt/SiO₂ than Pt/La_{0.5}Ce_{0.5}MnO₃ catalyst.

Discussion

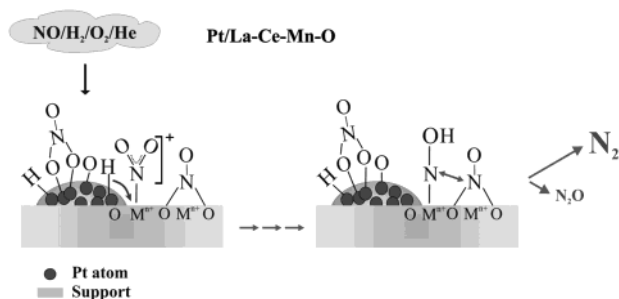
The purpose of this work was to study the essential mechanistic aspects of the $\text{NO}/\text{H}_2/\text{O}_2$ lean de- NO_x catalytic reaction over the 0.1 wt % Pt/La_{0.5}Ce_{0.5}MnO₃ solid that exhibits remarkable catalytic behavior,⁹ namely nitrogen selectivity values greater than 80% in the 100–400 $^\circ\text{C}$ range (5% H_2O in the feed) and a wide reaction-temperature-window of operation compared to the conventional 0.1 wt % Pt/SiO₂ catalyst.⁹ This is in an effort to gather fundamental information about the intrinsic reasons for such support effects in the catalytic behavior of supported-Pt solids for the present reaction system. The most

**Figure 7.** Transient response curves of N_2^{16}O , N_2^{18}O , and Ar obtained following the isotopic switch $\text{NO}/\text{H}_2/^{16}\text{O}_2/\text{Ar}/\text{He} \rightarrow \text{NO}/\text{H}_2/^{18}\text{O}_2/\text{He}$ at 140 $^\circ\text{C}$ (expt. C, Table 1) over the 0.1 wt % Pt/La_{0.5}Ce_{0.5}MnO₃ (a) and 0.1 wt % Pt/SiO₂ (b) catalysts. Feed gas composition: $\text{H}_2 = 1.0\%$, $\text{NO} = 0.25\%$, $\text{O}_2 = 2\%$, $\text{Ar} = 1\%$, He as balance gas.

appropriate technique for in situ mechanistic studies of gas–solid heterogeneous catalytic reactions, that of SSITKA^{19–21} with mass spectrometry and FTIR as detectors, has been used in the present work.

The differences in the DRIFTS spectra (Figures 1–3), SSITKA transient response curves (Figures 4, 5, and 7), and H_2 TPSR profiles (Figure 6) obtained over the two catalyst formulations investigated reflect the dependence of chemical structure and reactivity of adsorbed NO_x species on support chemical composition. The in situ DRIFTS/SSITKA (use of ^{15}NO) experiments (Figures 1–3) have demonstrated that on the Pt/La_{0.5}Ce_{0.5}MnO₃ catalyst there exist two active NO_x intermediate species. These are nitrosyls on the support (IR band at 2220 cm^{-1}), which do not exchange with gaseous NO (irreversibly chemisorbed NO_x species), and bidentate nitrates on the support (IR band at 1540 cm^{-1}) which are also irreversibly chemisorbed. The concentration of these two species, as determined by SSITKA experiments using mass spectrometer as detector (Figure 4), was found to be 8.1 $\mu\text{mol/g}$ ($\theta = 1.8$). On the other hand, other adsorbed NO_x species are formed during $\text{NO}/\text{H}_2/\text{O}_2$ reaction at 140 $^\circ\text{C}$ but they do not participate (spectator species) in the formation of N_2 and N_2O . The chemical structure of these NO_x species has been presented in the result section. Among the inactive NO_x species, only the unidentate nitrate on Pt (IR band at 1520 cm^{-1}) was found to be a reversibly chemisorbed species (exchangeable NO_x species, Figure 3a). The amount of inactive NO_x species (spectator species) accumulated on the catalyst surface after 30 min of

SCHEME 2: Illustration of the Site Population and Interaction of the Two Active Adsorbed Precursor Intermediate NO_x Species Formed on Pt/La_{0.5}Ce_{0.5}MnO₃ that Lead to N₂ and N₂O Formation



SCHEME 3: Illustration of the Site Population and Interaction of the Two Active Adsorbed Precursor Intermediate NO_x Species Formed on Pt/SiO₂ that Lead to N₂ and N₂O Formation



will require the spillover of active atomic hydrogen species formed on Pt to this metal–support interface region (Scheme 1).

Scheme 2 illustrates essential key aspects of the mechanistic steps involved in the reaction system at hand in the case of Pt/La_{0.5}Ce_{0.5}MnO₃ catalyst. A plausible mechanistic step for the reduction of the two active NO_x species located within the zone of the metal–support interface as previously discussed (see Scheme 1) is suggested to be the hydrogen spillover from the Pt to the support surface. Such a mechanism was recently supported by experimental results of NO_x reduction by hydrogen in the case of Pd/MnO_x-CeO₂ catalyst.¹¹ Note the large similarity of the latter support with the present support composition of La_{0.5}Ce_{0.5}MnO₃. As indicated by the SSITKA experiments performed over the Pt/La_{0.5}Ce_{0.5}MnO₃ catalyst (Figure 4), the interaction of the two active NO_x species favors the formation of N₂ than N₂O in harmony with the high N₂ reaction selectivity values obtained for the present catalytic system.⁹ Maunula et al.⁵¹ have studied the NO/H₂ reaction mechanism over a 0.2 wt %Pt/CeO₂-Al₂O₃ catalyst with the use of various transient experiments. The authors reported that an active intermediate NO_x species of the NO/H₂ reaction is likely the (NO)₂ dimer designated as *NO••NO*.⁵¹ This can lead either to adsorbed N₂O and atomic oxygen or to N₂ and atomic oxygen. In the present work, a similar mechanism is proposed (Scheme 2) where the two active NO_x species are of different chemical structure and located not on the Pt metal but on the support surface.

Scheme 3 illustrates the essential aspects of the mechanistic steps involved in the reaction at hand in the case of Pt/SiO₂ catalyst. For this catalyst, both active NO_x species were found to be located on Pt, where one of them (Pt–NO^{δ+}) is reversibly chemisorbed. The formation of N₂ proceeds with the participa-

tion of both kinds of NO_x species as clearly demonstrated in Figures 5a and 6b (¹⁴N¹⁵N transient response). In Schemes 2 and 3 the composition of the various intermediate species along the reaction path from NO_x precursor species to the final N₂ and N₂O gas products cannot be determined from the present work.

Burch et al.^{26,27,30} have studied the mechanism of the NO/H₂ and NO/H₂/O₂ reactions over a Pt/SiO₂ catalyst by using the SSITKA technique. The authors have suggested that the formation route of N₂ in an extent of 85% is the result of the interaction of two different NO_x species, whereas that of N₂O is a result of two similar in nature NO_x species.³⁰ It should be noticed that neither the chemical structure of the active NO_x species nor the chemical structure and composition of the inactive NO_x (spectator species) have been determined.³⁰ However, several aspects of the mechanism of N₂ formation over the Pt/SiO₂ catalyst suggested by Burch et al.³⁰ find strong support from the results of the present work. These are the following:

(1) The main route of N₂ formation involves indeed the interaction of two active NO_x species different in chemical structure. Their structure is identified for the first time in the present work (nitrosyls and unidentate nitrates adsorbed on Pt).

(2) One of the two NO_x species required for the formation of N₂ has been suggested by Burch et al.³⁰ to be a weakly chemisorbed NO species (named NO_{preads}). The present work has illustrated that this species is the nitrosyl one that easily exchanges with gaseous ¹⁵NO. The second NO_x species, named NO_{ads} by Burch et al.³⁰ provides a reduced NH_x (x = 0–2) species that recombines with NO_{preads} to form N₂. This second NO_x species is the unidentate nitrate as identified for the first time in the present work.

(3) The surface coverage of the active NO_x intermediate species that lead to the N₂ production is considerably larger than that leading to N₂O.

(4) The surface of Pt is not fully covered with N-containing species. Burch et al.³⁰ proposed that NO-derived spectator species can be stable under reaction conditions. This is indeed what has been revealed for the first time in the present work. The unidentate nitrate on Pt (IR band at 1620 cm⁻¹) is found not to be active NO_x intermediate species.

It is also important to illustrate some discrepancies in other mechanistic aspects revealed after comparing the SSITKA results reported by Burch et al.³⁰ and the present ones. These are the following:

(1) The immediate production of ¹⁴N¹⁵NO and the non existence of any ¹⁴N₂O upon the isotopic switch (Figure 5b), and the same position in time of the peak maximum observed in the transient response curves of ¹⁴N¹⁵N and ¹⁴N¹⁵NO may suggest that the same active NO_x precursor species must be involved in both N₂ and N₂O formation pathways. The very fast exchange of adsorbed nitrosyls with ¹⁵NO(g) and the reaction of it with the nonexchangeable unidentate nitrate explain very well the observed transient response of ¹⁴N¹⁵NO. On the contrary, Burch et al.³⁰ have proposed that N₂O formation passes through a dimeric (NO)₂ intermediate species derived from two similar NO_{preads} species.

Snis and Panas⁴⁴ and Acke et al.^{52–54} have studied in detail the various surface complexes of NO formed on the surface of alkaline metal oxides in an oxidized and reduced state and also the role of the (NO)₂ dimer toward the production of N₂O and N₂ gas products. A main conclusion from these works is that a possible reaction channel for N₂O formation is that which involves the (NO)₂ dimer. This species (negatively charged) can

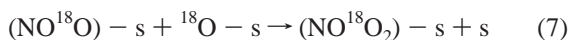
be formed either on metal cationic sites or on oxygen vacancies. For the latter case, a prereduced metal oxide surface is required. In the present work, the NO/H₂/O₂ reaction was investigated at the low-temperature of 140 °C and in strongly oxidizing conditions (5% O₂ and 1% H₂ in the feed stream). It is, therefore, not logical to suggest that N₂O₂ⁿ⁻ species associated with oxygen vacant sites can be populated on the present CeO₂, LaMnO₃, and MnO₂ support metal oxide surfaces. On the other hand, N₂O₂ⁿ⁻ adsorbed species associated with metal cations of the above-mentioned metal oxides is possible according to Table 2 and the DRIFTS results of Figure 1a. However, these species were not found to be active NO_x precursor species according to the DRIFTS/SSITKA results of Figure 2a. The latter results are the most convincing ones to exclude the latter species of being considered as an active intermediate species of the present catalytic reaction at the experimental conditions investigated.

In the case of formation of the (NO)₂ dimer on a metal surface, it has been reported^{55–57} that in order this weakly bound species to be dissociated into N₂O and atomic oxygen, an electron transfer from the substrate to the (NO)₂ dimer is necessary for breaking the strong N–N bond. In fact, this reaction channel has been observed on Ag(111) and Cu (111) surfaces^{55–57} even at temperatures as low as –198 °C.

The relatively larger reaction temperature of 140 °C and the higher Pt dispersion (90%) used in the present work compared to 60–83 °C and 30%, respectively, used in the work of Burch et al.,³⁰ and the feed gas composition of 1.64% NO, 1.64% H₂ and 8.7% O₂ used in the latter work could be reasons that (NO)₂ dimer on Pt is not an active NO precursor to form N₂O in the present catalytic system.

(2) In the present work, the transient evolution of the N₂O isotopic species with time on stream after the isotopic switch was made (Figure 5) appears very similar to that of the N₂ isotopic species. In the work of Burch et al.,³⁰ it was shown that N₂O isotopic species were evolved first compared to the corresponding N₂ ones. This difference again seems to be the result of the different kinetics and mechanism operated in the two Pt/SiO₂ catalysts investigated at different reaction conditions as previously discussed.

The ¹⁸O₂ SSITKA experiments (Figure 7) performed over the Pt/SiO₂ and Pt/La_{0.5}Ce_{0.5}MnO₃ catalysts provide very important mechanistic information about the oxygen pathway of the N₂O formation route in the NO/H₂/O₂ reaction. The results obtained show that participation of gaseous O₂ in the N₂O formation route is more substantial on Pt/SiO₂ than Pt/La_{0.5}Ce_{0.5}MnO₃ catalyst. In particular, it was found that on Pt/SiO₂ catalyst about 17% of the total oxygen (O atoms) that participates in the reaction mechanism of N₂O formation originates from the gas-phase oxygen species, whereas the rest of it originates from the NO reactant molecule. On the contrary, the respective percentage over the Pt/La_{0.5}Ce_{0.5}MnO₃ catalyst was found to be two times smaller. The gas phase ¹⁸O₂ can participate in the reaction route of N₂O formation through the oxidation of adsorbed NO on Pt to form various nitrite and nitrate species, according to the following elementary reaction steps (eqs 5–7):^{58,59}



where s is a surface Pt atom. As previously mentioned, the active

precursor intermediate NO_x species that lead to the formation of N₂ and N₂O during NO/H₂/O₂ reaction conditions over the Pt/SiO₂ catalyst are Pt–NO^{δ+} and Pt–NO₃. The latter species is formed after oxidation of the adsorbed NO on Pt, according to eqs 5–7. Reduction of these species by atomic hydrogen leads to N₂ and N₂O according to Scheme 3.

On the contrary, the active precursor intermediate NO_x species that lead to the formation of N₂ and N₂O over the Pt/La_{0.5}Ce_{0.5}MnO₃ catalyst are the M–NO⁺ and/or M–NO₂⁺ (Table 2) and M–O–(NO)–O–M (where M is the metal cation of the support). It has been suggested⁶⁰ that the M–NO⁺ is first formed after direct adsorption of NO on two oxygen atoms of the support, followed by surface transformation into an adsorbed NO⁺ species on the adjacent metal cation. The participation of gaseous oxygen in the formation route of the latter species is considered less possible than that described by eqs 5–7 because it would assume the direct exchange of the surface oxygen atoms of support with the ones of the gas phase dioxygen. The latter process is known to be significantly activated,⁶¹ and thus, the respective rate is expected to be very small at 140 °C. Therefore, the only possibility to form N₂¹⁸O as observed in the SSITKA experiment (Figure 7a) is via oxidation of NO on Pt (see eqs 5 and 6), formation of gaseous N¹⁶O¹⁸O followed by adsorption on a metal cation of the support (M–NO₂⁺ species). The latter species is then reduced by H₂ into N₂¹⁸O. It appears, therefore, that NO₂ is an intermediate species in the N-pathway of N₂O formation over Pt/La_{0.5}Ce_{0.5}MnO₃ catalyst. However, the presence of M–NO⁺ cannot be excluded (see Table 2).

According to the discussion offered previously, an explanation of why Pt/La_{0.5}Ce_{0.5}MnO₃ presents much higher N₂ reaction selectivity values than the Pt/SiO₂ catalyst^{8,9} could be as follows. The selective reduction of nitrosyl and unidentate nitrate species to N₂ on Pt/SiO₂ seems to require sufficient surface coverage of hydrogen (θ_H) than in the case of Pt supported on La_{0.5}Ce_{0.5}MnO₃. The H₂ TPSR experiment shown in Figure 6b strongly supports this view. Even though the coverage of active NO_x intermediate species in the case of Pt/SiO₂ is of the order of 0.6–0.7 of a monolayer (Table 3), adsorbed inactive bidentate nitrates on Pt (Figure 1b) and expected atomic oxygen species leave little sites for hydrogen chemisorption. On the contrary, in the case of the Pt/La_{0.5}Ce_{0.5}MnO₃ catalyst, the operative reaction step of hydrogen spillover and the abundant concentration of sites for hydrogen accommodation on the support (M–O + H → M–OH) gives rise to an increased rate of reduction of NO_x species to N₂ than N₂O gas product. On the other hand, it should be mentioned that the relative strength of the N–O bond in the various active NO_x species identified in the two supported-Pt catalysts must be considered as an important factor that controls the relative rates of N₂ formation in the two catalysts.

Conclusions

The following conclusions can be derived from the results of the present work:

1. The ¹⁵NO SSITKA/FTIR combined with H₂ TPSR isotopic experiments have illustrated that the N-pathway from gaseous NO to N₂ formation in the NO/H₂/O₂ reaction at 140 °C over the Pt/La_{0.5}Ce_{0.5}MnO₃ and Pt/SiO₂ catalysts passes through two different in chemical structure NO_x adsorbed precursor intermediate species.

2. In the case of the Pt/La_{0.5}Ce_{0.5}MnO₃ catalyst, the active NO_x species (M–NO₂⁺ and M–O–(NO)–O–M) are populated on the metal–support inter-phase region. On the contrary, in the case of Pt/SiO₂, the active NO_x adsorbed intermediate species are populated on the Pt metal surface (Pt–NO^{δ+} and Pt–NO₃).

3. The N-pathway that gaseous NO follows to form N₂O in the NO/H₂/O₂ reaction includes the same active NO_x precursor intermediate species that eventually lead also to N₂ gas product. The mechanism of the NO/H₂/O₂ lean de-NO_x reaction over the 0.1 wt % Pt/La_{0.5}Ce_{0.5}MnO₃ catalyst must include a H-spillover process from the Pt metal to the La_{0.5}Ce_{0.5}MnO₃ support surface.

4. In the case of the Pt/SiO₂ catalyst, the surface coverage of H (θ_H) seems to control the N₂ reaction selectivity.

5. The surface pool of active NO_x species that eventually lead to the formation of N₂ is found to be significantly larger than the surface NO_x pool that leads to the formation of N₂O.

6. The ¹⁸O₂ SSITKA experiments have shown that the NO/H₂/O₂ reaction toward N₂O formation involves a reaction path of NO oxidation on Pt with the participation of gaseous oxygen. This route is more important on Pt/SiO₂ than on the Pt/La_{0.5}Ce_{0.5}MnO₃ catalyst.

7. Inactive NO_x species accumulate on Pt after 30 min of NO/H₂/O₂ reaction at 140 °C over both Pt/La_{0.5}Ce_{0.5}MnO₃ and Pt/SiO₂ catalysts. Their chemical structure, however, is different for each catalyst formulation.

Acknowledgment. The financial support of the Research Committee of the University of Cyprus through a competitive research grant is gratefully acknowledged.

References and Notes

- Burch, R.; Millington, P. J.; Walker, A. P. *Appl. Catal. B: Environ.* **1994**, *4*, 160.
- Centi, G. *J. Mol. Catal. A: Chem.* **2001**, *173*, 287.
- Yokota, K.; Fukui, M.; Tanaka, T. *Appl. Surf. Sci.* **1997**, *121/122*, 273.
- Machida, M.; Ikeda, S.; Kurogi, D.; Kijima, T. *Appl. Catal. B: Environ.* **2001**, *35*, 107.
- Frank, B.; Emig, G.; Renken, A. *Appl. Catal. B: Environ.* **1998**, *19*, 45.
- Burch, R.; Coleman, M. D. *Appl. Catal. B: Environ.* **1999**, *23*, 115.
- Ueda, A.; Nakao, T.; Azuma, M.; Kobayashi, T. *Catal. Today* **1998**, *45*, 135.
- Costa, C. N.; Savva, P.; Andronikou, C.; Lambrou, P.; Polychronopoulou, K.; Belessi, V. C.; Stathopoulos, V. N.; Pomonis, P. J.; Efstathiou, A. M. *J. Catal.* **2002**, *209*, 456.
- Costa, C. N.; Stathopoulos, V. N.; Belessi, V. C.; Efstathiou, A. M. *J. Catal.* **2001**, *197*, 350.
- Pereira, C. J.; Phumlee, K. W. *Catal. Today* **1992**, *13*, 23.
- Machida, M.; Kurogi, D.; Kijima, T. *J. Phys. Chem. B* **2003**, *107*, 196.
- Satokawa, S.; Shibata, J.; Shimizu, K.; Satsuma, A.; Hattori, T. *Appl. Catal. B: Environ.* **2003**, *42*, 179.
- Kokes, R. J. *J. Phys. Chem.* **1966**, *70*, 296.
- Kobylinski, T. P.; Taylor, B. W. *J. Catal.* **1973**, *33*, 376.
- Hodjati, S.; Bernhardt, P.; Petit, C.; Pitchon, V.; Kinennemann, A. *Appl. Catal. B: Environ.* **1998**, *19*, 221.
- Lietti, L.; Forzatti, P.; Nova, I.; Tronconi, S. *J. Catal.* **2001**, *204*, 175.
- Takahashi, N.; Shinjo, H.; Iiyama, T.; Suzuki, T.; Yamazaki, K.; Yokota, K.; Suzuki, H.; Miyoshi, N.; Matsumoto, S.; Tanizawa, T.; Tanaka, T.; Tateishi, S.; Kasahara, K. *Catal. Today* **1996**, *27*, 63.
- Busca, G.; Lietti, L.; Ramis, G.; Berti, F. *Appl. Catal. B: Environ.* **1998**, *18*, 1.
- Efstathiou, A. M.; Verykios, X. E. *Appl. Catal. A: General* **1997**, *151* (1), 109.
- Shannon, S. L.; Goodwin, J. G. *Chem. Rev.* **1995**, *95*, 677.
- Mirodatos, C. *Catal. Today* **1991**, *9*, 83.
- Happel, J. In *Isotopic Assessment of Heterogeneous Catalysis*; Academic Press: New York, 1986.
- Bennett, C. O. *Adv. Catal.* **2000**, *44*, 329.
- Efstathiou, A. M.; Fliatoura, K. *Appl. Catal. B: Environ.* **1995**, *6* (1), 35.
- Kumthekar, M. W.; Ozkan, U. S. *J. Catal.* **1997**, *171* (1), 54.
- Burch, R.; Sullivan, J. A. *J. Catal.* **1999**, *182* (2), 489.
- Burch, R.; Shestov, A. A.; Sullivan, J. A. *J. Catal.* **1999**, *182* (2), 497.
- Burch, R.; Shestov, A. A.; Sullivan, J. A. *J. Catal.* **1999**, *186*, 353.
- Shestov, A. A.; Burch, R.; Sullivan, J. A. *J. Catal.* **1999**, *186*, 362.
- Burch, R.; Shestov, A. A.; Sullivan, J. A. *J. Catal.* **1999**, *188*, 69.
- Gatica, J. M.; Baker, R. T.; Fornasiero, P.; Bernal, S.; Kašpar, J. *J. Phys. Chem. B* **2001**, *105*, 1191.
- Costa, C. N.; Anastasiadou, T.; Efstathiou, A. M. *J. Catal.* **2000**, *194*, 250.
- Costa, C. N.; Christou, S. Y.; Georgiou, G.; Efstathiou, A. M. *J. Catal.* **2003**, *219*, 259.
- Levy, P. J.; Pitchon, V.; Perrichon, V.; Primet, M.; Chevrier, M.; Gauthier, C. *J. Catal.* **1998**, *178*, 363.
- Rogemond, E.; Essayem, N.; Frety, R. V.; Perrichon, V.; Primet, M.; Chevrier, M.; Gauthier, C.; Mathis, F. *J. Catal.* **1999**, *186*, 414.
- Hoost, T. E.; Otto, K.; Laframboise, K. A. *J. Catal.* **1995**, *155*, 303.
- Freys, J.-L.; Saussey, J.; Lavalley, J.-C.; Bourges, P. *J. Catal.* **2001**, *197*, 131.
- Garin, F. *Appl. Catal. A* **2001**, *222*, 183.
- Morrow, B. A.; Chevrier, J. P.; Moran, L. E. *J. Catal.* **1985**, *91*, 208.
- Levoguer, C. L.; Nix, R. M. *Surf. Sci.* **1996**, *365*, 672.
- Ryczkowski, J. *Catal. Today* **2001**, *68*, 263.
- Binet, C.; Daturi, M.; Lavalley, J.-C. *Catal. Today* **1999**, *50*, 207.
- Huang, S.-J.; Walters, A. B.; Vannice, M. A. *Catal. Lett.* **2000**, *64*, 77.
- Snis, A.; Panas, I. *Surf. Sci.* **1998**, *412/413*, 477.
- Yanagisawa, Y. *Appl. Surf. Sci.* **1996**, *100/101*, 256.
- Beutel, T.; Adelman, B. J.; Sachtler, W. M. H. *Appl. Catal. B: Environ.* **1996**, *9*, L1.
- Fritz, A.; Pitchon, V. *Appl. Catal. B: Environ.* **1997**, *13*, 1.
- Primet, M.; Basset, J. M.; Garbowski, E.; Mathieu, M. V. *J. Am. Chem. Soc.* **1975**, *97*, 3655.
- Solymosi, F.; Knözinger, H. *J. Chem. Soc., Faraday Trans.* **1990**, *86* (2), 389.
- Ioannides, T.; Verykios, X. E. *J. Catal.* **1996**, *161*, 560.
- Maunula, T.; Ahola, J.; Salmi, T.; Haario, H.; Harkonen, M.; Luoma, M.; Pohjola, V. *Appl. Catal. B: Environ.* **1997**, *12*, 287.
- Acke, F.; Panas, I. *J. Phys. Chem. B* **1999**, *103*, 2195.
- Acke, F.; Skoglundh, M. *J. Phys. Chem. B* **1999**, *103*, 972.
- Acke, F.; Panas, I.; Strömberg, D. *J. Phys. Chem. B* **1997**, *101*, 6484.
- Brown, W. A.; Gardner, P.; Perez-Jigato, M.; King, D. A. *J. Chem. Phys.* **1995**, *102*, 7277.
- Brown, W. A.; Gardner, P.; King, D. A. *J. Phys. Chem.* **1995**, *99*, 7065.
- Dumas, P.; Suhren, M.; Chabal, Y. J.; Hirschmugl, J. C.; Williams, G. P. *Surf. Sci.* **1997**, *371*, 200.
- Hasse, G.; Asscher, M. *Surf. Sci.* **1987**, *191*, 75.
- Olsson, L.; Fridell, E. *J. Catal.* **2002**, *210*, 340.
- Klingerberg, B.; Vannice, M. A. *Chem. Mater.* **1996**, *8*, 2755.
- Dabrowski, A. *Adv. Colloid Interface Sci.* **2001**, *93*, 135.